Search for quantum gravity with IceCube and high energy atmospheric neutrinos

Warren Huelsnitz* **and John Kelley**† **for the IceCube Collaboration**‡

*Department of Physics, University of Maryland, College Park, MD 20742, USA
†Department of Physics, University of Wisconsin, Madison, WI 53706, USA
‡See the special section of these proceedings

***Abstract*. We present the expected sensitivity of an analysis that will use data from the IceCube Neutrino Observatory to search for distortions in the energy or directional dependence of atmospheric neutrinos. Deviations in the energy and zenith angle distributions of atmospheric neutrinos due to Lorentz invariance violation or quantum decoherence could be a signature of quantum gravity in the neutrino sector. Additionally, a periodic variation as a function of right ascension is a possible consequence of a Lorentz-violating preferred frame. We use a likelihood method to constrain deviations in the energy and zenith angle distributions and a discrete Fourier transform method to constrain a directional asymmetry in right ascension. In the absence of new physics, the likelihood method can also constrain conventional and prompt atmospheric neutrino flux models. Results from a similar analysis using data from the AMANDA-II detector are also discussed.**

***Keywords*: quantum gravity, Lorentz violation, atmospheric neutrinos**

I. Introduction

Physicists have so far been unable to reconcile quantum field theory and general relativity into a coherent theory of quantum gravity (QG). Numerous approaches are in development, and common to many is the possibility that Lorentz invariance is violated at extremely small distance scales (high energy scales), due to a discrete structure of spacetime or an invariant minimum length scale. Interactions with a spacetime foam, or virtual black holes, may also induce quantum decoherence in which pure quantum states evolve into mixed states [1].

Neutrinos, lacking any gauge interactions other than weak, and having extremely high Lorentz factors, are sensitive probes of these effects. Violation of Lorentz invariance (VLI) can induce a number of flavor-changing signatures in neutrinos, including oscillations with unique energy dependencies or directional asymmetries due to a Lorentz-violating preferred frame. Quantum decoherence (QD) can also result in flavor-changing effects that depend upon the neutrino energy.

Atmospheric neutrinos are produced in the decay chains of particles resulting from the interaction of cosmic rays with the earth's atmosphere [2,3]. The IceCube neutrino telescope [4], currently under construction in the glacial ice at the South Pole, detects the Cherenkov radiation emitted by charged particles produced by neutrino interactions in the ice or rock. IceCube has already collected a large sample of atmospheric muon neutrinos in the energy range of 100 GeV to a few tens of TeV, and can search for deficits caused by possible QG effects such as VLI or QD.

We will first review the phenomenological models of QG to be tested. Then, we will discuss event selection and the observables used for the analysis, followed by a discussion of the likelihood and discrete Fourier transform (DFT) methods we use. Finally, results from the AMANDA-II detector, and expected sensitivity of the 40-string configuration of IceCube will be discussed.

II. Phenomenology

A. Violation of Lorentz Invariance

For VLI models, we consider the case of a flavor-dependent dispersion relation, or, equivalently, flavor-dependent limiting velocities that differ from the speed of light [5, 6]. Further, we make the simplifying assumption of a two neutrino model in which the new eigenstates are characterized by a mixing angle ξ and a phase η. This leads to a muon neutrino survival probability of the form:

$$P_{\nu_\mu\to\nu_\mu} = 1 - \sin^2 2\Theta \sin^2\left(\frac{\Delta m^2 L}{4E}\Re\right).$$

E is the neutrino energy and L the propagation distance for the atmospheric neutrino, which is a function of zenith angle. Θ is the effective mixing angle, given by

$$\sin^2 2\Theta = \left(\sin^2 2\theta + R^2\sin^2 2\xi + 2R\sin 2\theta\sin 2\xi\cos\eta\right)\big/\Re^2.$$

The effective oscillation wavelength is

$$\Re = \left(1 + R^2 + 2R\left[\cos 2\theta\cos 2\xi + \sin 2\theta\sin 2\xi\cos\eta\right]\right)^{-1/2}.$$

R is the ratio between the VLI oscillation wavelength and the mass-induced oscillation wavelength:

$$R = \frac{\Delta c}{c}\frac{E}{2}\frac{4E}{\Delta m^2}.$$

$\Delta c/c$ is the velocity splitting between eigenstates. The VLI oscillation length can be generalized to integral powers of neutrino energy:

$$\frac{\Delta c}{c}\frac{LE}{2} \rightarrow \Delta\delta\frac{LE^n}{2}.$$

Since mass-induced oscillations are suppressed in the energy range for this analysis, we can make a simplifying assumption and set $\eta = \pi/2$ so that $\cos\eta = 0$. We then have two physics parameters: $\Delta c/c$ and $\sin^2 2\xi$.

B. Decoherence

For quantum decoherence, we use a full three-neutrino model, in which the muon neutrino survival probability can be written [7, 8]:

$$\begin{aligned} P_{\nu_\mu\rightarrow\nu_\mu} = \frac{1}{3} + \frac{1}{2}\{ & e^{-\gamma_3 L}\cos^4\theta_{23} \\ & + \frac{1}{12}e^{-\gamma_8 L}\left(1 - 3\cos 2\theta_{23}\right)^2 \\ & + 4e^{\frac{-(\gamma_6+\gamma_7)L}{2}}\cos^2\theta_{23}\sin^2\theta_{23} \\ & \times \left[\cos\left(L\sqrt{m}/2\right)\right. \\ & + \left.\sin\left(L\sqrt{m}/2\right)(\gamma_6 - \gamma_7)/\sqrt{m}\right]\}, \end{aligned} \tag{1}$$

$$\text{with } m \equiv \left|(\gamma_6 - \gamma_7)^2 - \left(\Delta m_{23}^2/E\right)^2\right|.$$

To limit the number of physics parameters, we assume that $\gamma_3 = \gamma_8$ and $\gamma_6 = \gamma_7$. The γ_i can be generalized to integral powers of neutrino energy:

$$\gamma_i \rightarrow \gamma_i^*\left(\frac{E}{\text{GeV}}\right)^n \text{GeV}.$$

The units of γ_i^* are then GeV^{-n+1}.

C. Directional Asymmetry

The location of IceCube at the South Pole is ideally suited to search for a sidereal variation in the flux of atmospheric neutrinos. Right ascension (RA) is synonymous with sidereal phase, and azimuthal asymmetries in the detector average out over a year. We use a two-neutrino model derived from the Standard Model Extension (SME), known as the vector model [9]. This model predicts a survival probability that depends on the direction of neutrino propagation:

$$\begin{aligned} P_{\nu_\mu\rightarrow\nu_\mu} = 1 - \sin^2\Big(L\Big[& (A_s)_{\mu\tau}\sin(\alpha+\varphi_0) \\ & + (A_c)_{\mu\tau}\cos(\alpha+\varphi_0)\Big]\Big). \end{aligned}$$

α is the RA of the neutrino and φ_0 is the offset between the origin of our coordinate system and a 'preferred' direction. A_s and A_c are functions of neutrino energy, E, neutrino direction unit vectors, $\hat{N}$, and four coefficients from the SME, the $(a_L)^\mu$ and $(c_L)^{\mu\nu}$:

$$(A_s)_{\mu\tau} = \hat{N}^Y\left(a_L^X - 2Ec_L^{TX}\right) - \hat{N}^X\left(a_L^Y - 2Ec_L^{TY}\right),$$

$$(A_c)_{\mu\tau} = -\hat{N}^X\left(a_L^X - 2Ec_L^{TX}\right) - \hat{N}^Y\left(a_L^Y - 2Ec_L^{TY}\right).$$

Typically, we assume $a_L^X = a_L^Y$ and $c_L^{TX} = c_L^{TY}$ in the analysis. Additionally, while constraining the a_L coefficients, the c_L are set to 0, and when constraining the c_L coefficients, the a_L are set to 0.

III. Event Selection

We are interested in upgoing atmospheric ν_μ events, and the main background is cosmic-ray muons. Even after an initial event selection based on zenith angle, the event sample is dominated, by several orders of magnitude, by misreconstructed cosmic-ray muons. This background is further reduced by event selection cuts that are based on track quality parameters and on fits to alternative track hypotheses. Alternative track hypotheses include downgoing versus upgoing tracks, and coincident muon events.

Since the remaining background contamination is difficult to model with simulation, we require an essentially pure neutrino sample. Final event selection to achieve this level of purity is done using a Boosted Decision Tree (BDT) [10]. The event sample for one year of data from 40-string IceCube is expected to be about 20,000 upgoing neutrinos, with zenith angles between 90 and 180 degrees, and neutrino energies from 100 GeV to about 30 TeV.

IV. Flux Modeling and Binning

Simulated events are weighted by their contribution to conventional [2, 3] and prompt [11–13] atmospheric neutrino flux models. These weights are then multiplied by the applicable oscillation or decoherence survival probability. Nuisance parameters are used in the likelihood analysis to account for the more significant theoretical and experimental uncertainties in flux normalization, spectral index, and zenith angle distribution. Individual events are thus weighted as follows:

$$w = A\left\{Bw_{conv} + Cw_{prompt}\right\}P_{\nu_\mu\rightarrow\nu_\mu},$$

where

$$A = \varepsilon\left(\frac{E}{1\text{ TeV}}\right)^{\Delta\gamma}\left[1 + 2\alpha\left(\cos\theta_Z + {}^1\!/_2\right)\right],$$

$$B = \left[1 + 2\alpha_c\left(\cos\theta_Z + {}^1\!/_2\right)\right], \text{ and}$$

$$C = A_p\left(\frac{E}{5\text{ TeV}}\right)^{\Delta\gamma_p}.$$

ε accounts for theoretical and experimental uncertainties in the overall flux normalization, such as ice model uncertainties, optical module (OM) sensitivity uncertainty, interaction rate uncertainties, reconstruction errors, etc. $\Delta\gamma$ accounts for the uncertainty in the primary cosmic ray slope as well as the impact of OM and ice model uncertainties on the observed spectral index. α accounts for the impact of OM and ice model uncertainties on the zenith angle tilt of the observed flux. α_c accounts for theoretical uncertainty in the zenith-angle tilt of the conventional atmospheric neutrino flux, primarily due to uncertainty in the pion to kaon ratio. A_p and $\Delta\gamma_p$ account for theoretical uncertainty in the magnitude and spectral index of the prompt atmospheric neutrino flux, primarily due to uncertainties in charm production cross sections and fragmentation functions.

θ_Z is the zenith angle of the neutrino, and $P_{\nu_\mu \to \nu_\mu}$ is the oscillation or decoherence survival probability. The particular forms of the spectral tilt and zenith angle tilt equations were chosen to minimize the impact on overall normalization as the correction factors are varied.

Events are binned in $\log_{10}(dE/dX)$ and $\cos(\theta_Z)$ for tests of VLI, decoherence, and atmospheric flux models, and in RA for the vector model. dE/dX, with units of GeV m^{-1}, is the average energy loss per unit propagation length of a muon that would produce the detected amount of light, and serves as an estimator for the original neutrino energy. The energy resolution is about 0.3 on a log scale, reducing sensitivity to VLI effects by a factor of two as compared to perfect energy resolution. Histograms for $\log_{10}(dE/dX)$ and $\cos(\theta_Z)$ are 10 x 10, and range from -1.9 to 1.1 for $\log_{10}(dE/dX)$ and -1 to 0 for $\cos(\theta_Z)$. 32 bins, from 0 to 360°, are used for RA, and include events in the declination band 0 to -30° (zenith band 90 to 120°).

Since some of the ν_μ are assumed to oscillate to ν_τ, ν_τ-induced muons are included in the simulation chain. Finally, bin counts for toy Monte Carlo (MC) histograms are varied according to Poisson distributions.

V. Likelihood Ratio Test

To determine the compatibility of various new physics hypotheses with the data and identify acceptance regions, we use a likelihood-ratio test and the ordering principle of Feldman and Cousins [14]. The signal we are looking for is a distortion, or a warping, of the event counts in the energy-zenith plane. A likelihood analysis takes advantage of this shape of the distribution and provides a convenient way to include systematic uncertainties in the overall normalization and shape of the atmospheric neutrino flux. Systematic uncertainties are included using the nuisance parameters discussed above, and the profile construction method [15,16]. The likelihood function is:

$$L\left(\{n_{ij}\}|\{\mu_{ij}\left(\theta_r, \theta_s\right)\}\right) = \prod_{i,j} \frac{\mu_{ij}^{n_{ij}}}{n_{ij}!} e^{-\mu_{ij}}.$$

n is the binned toy MC or real data and μ is the prediction. θ_r represents the physics parameters and θ_s the nuisance parameters. In practice, this function is maximized by finding the minimum of the negative log of the likelihood, using the Minuit2 package in ROOT [17]. The test statistic is the likelihood ratio,

$$R = -2\ln\frac{L_0}{\hat{L}}.$$

where L_0 is the maximum likelihood, i.e., the best fit to the data or the toy MC histogram, with physics parameters held fixed and nuisance parmaters allowed to vary over the ranges of their uncertainties. $\hat{L}$ is the maximum likelihood when physics as well as nuisance parameters are allowed to vary.

In the absence of new physics effects, the likelihood method will be used to evaluate theoretical uncertainties in conventional and prompt atmospheric neutrino flux models. For these analyses, experimental and theoretical uncertainties are split into separate nuisance parameters, and those associated with theoretical uncertainties in the conventional and/or prompt neutrino flux become physics parameters.

VI. DFT Analysis

Neutrino oscillations in the vector model depend on the x and y components of the neutrino propagation direction. Hence, a phase angle specifying the offset from a preferred direction is required. To conduct a model-independent search for a sidereal signal independent of an arbitrary assumption about this phase angle, we use a DFT analysis. This analysis is done in two stages and has been adapted from a similar analysis performed with the MINOS detector to search for a directional dependence [18]. In the first stage, the data is checked for consistency with the hypothesis of no sidereal signal. In the second stage, constraints are placed on the SME coefficients of the vector model.

First, a large number of toy experiments are performed in which the right ascensions of all events in the data are randomly redistributed. The power spectral densities (PSDs) in the $n = 1$ to $n = 4$ components of a DFT are computed for each of these 'noise-only' toy experiments. The corresponding frequencies are $n/T_\oplus$, where $T_\oplus$ is a sidereal day. The PSDs of the true data histogram are then computed and compared to the range of PSDs from the toy experiments. This indicates whether the data is consistent with the hypothesis of no sidereal signal.

In the vector model, muon neutrino survivial probability varies with RA with a modulation frequency of $4/T_\oplus$. To constrain the vector model, we look for an excess of power in the $n = 4$ harmonic. The energy and zenith angle distributions are modeled using simulated events and the best-fit nuisance parameter values from the data. A large number of toy MC experiments are created, using these best-fit values. The physics parameters of the vector model are then increased, and the simulated events reweighted accordingly, until a PSD greater than the 99th percentile of the PSDs from the noise-only toy experiments is obtained. The values found in each of these trials are then averaged to find the sensitivity of this analysis given the data and the absence of a signal.

VII. Results and Expectations

In a previous analysis of atmospheric muon neutrino events collected from 2000 to 2006 with the AMANDA-II detector [19], the data were consistent with the Standard Model, and upper limits on QG parameters were set. A VLI upper limit at the 90% CL was found of

$$\Delta c/c < 2.8 \times 10^{-27}$$

for VLI oscillations proportional to the neutrino energy. A QD upper limit at the 90% CL was found of

$$\gamma^* < 1.3 \times 10^{-31}\ \mathrm{GeV}^{-1}$$

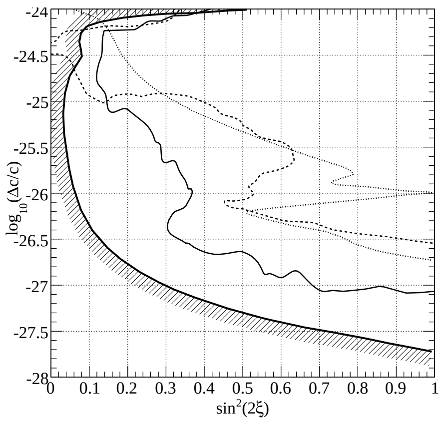

Fig. 1: VLI Model, 90% CL curves. Dashed: AMANDA-II [19]. Dotted: SuperK + K2K [5]. Solid with hash marks: expected 80-string IceCube sensitivity [6]. Solid: expected 40-string IceCube sensitivity (preliminary).

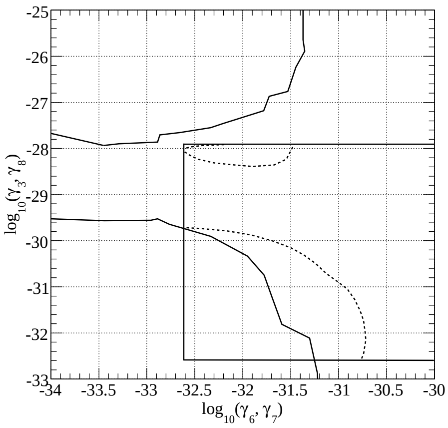

Fig. 2: Decoherence model, 90% CL curves. Dashed: AMANDA-II [19]. Solid: expected 40-string IceCube sensitivity (preliminary). The black box indicates region scanned in AMANDA-II analysis.

for decoherence effects proportional to E^2 and with all γ_i assumed equal. For one year of data from 40-string IceCube, we expect about a factor of three improvement:

$$\Delta c/c < 9.0 \times 10^{-28} \text{ and}$$

$$\gamma^* < 2.5 \times 10^{-32} \text{ GeV}^{-1}.$$

Figure (1) shows 90% CL curves for the $n = 1$ VLI model. Included are the AMANDA-II analysis, SuperK and K2K [5], and expected sensitivity for ten years of data from the full, 80-string, IceCube detector [6]. Also included is the 90% CL curve expected for the 40-string IceCube detector, based on a preliminary treatment of nuisance parameters. Figure (2) shows 90% CL curves for the $n = 2$ decoherence model from the AMANDA-II analysis, and the expected sensitivity for 40-string IceCube (also preliminary).

For the vector model, the sensitivity of the 40-string IceCube detector, at the 99% CL, is expected to be:

$$a_L^X = a_L^Y < 2.0 \times 10^{-23} \text{ GeV},$$
$$c_L^{TX} = c_L^{TY} < 6.6 \times 10^{-27}.$$

These limits are three orders of magnitude lower for the a_L terms and four orders of magnitude lower for the c_L terms than the limits reported in [18]. This is due to the longer baseline of atmospheric neutrinos, and higher energy reach of IceCube.

Data from AMANDA-II were used to find that the best-fit flux Φ for conventional atmospheric neutrinos, starting with the flux $(\Phi_{\rm Barr})$ of reference [2] is:

$$\Phi = (1.1 \pm 0.1) \left(\frac{E}{640 \text{ GeV}} \right)^{0.056} \Phi_{\rm Barr}.$$

This likelihood methodology will also be used with IceCube data to constrain conventional and prompt atmospheric neutrino flux models.

VIII. Conclusions

Data from IceCube's 40-string configuration will improve constraints on VLI and decoherence models beyond that achieved with AMANDA-II. Additionally, it will significantly improve constraints on a certain class of direction-dependent oscillation models.

The IceCube detector will be able to provide improved constraints on various models of quantum gravity and atmospheric neutrino flux models as the detector grows to its final design configuration and as data collection continues in the following years. The likelihood method and the flux weighting discussed above provide flexibility to adjust nuisance parameter ranges as IceCube systematic uncertainties become better constrained.

References

[1] S.W. Hawking, *Commun. Math. Phys.*, 87:395 (1982).
[2] G.D. Barr *et al.* , *Phys. Rev. D.*, 70:023006 (2004).
[3] M. Honda *et al.* , *Phys. Rev. D.*, 75:043006 (2007).
[4] A. Karle, *arXiv:0812.3981v1*.
[5] M.C. Gonzalez-Garcia and M. Maltoni, *Phys. Rev. D.*, 70:033010 (2004).
[6] M.C. Gonzalez-Garcia, F. Halzen and M. Maltoni, *Phys. Rev. D.*, 71:093010 (2005).
[7] A.M. Gago *et al.* , *arXiv:hep-ph/0208166v1*.
[8] L. Anchordoqui and F. Halzen, *Annals Phys.*, 321:2660 (2006).
[9] V.A. Kostelecky and M. Mewes, *Phys. Rev. D.*, 70:076002 (2004).
[10] A. Hocker *et al.* , *arXiv:physics/0703039v4*.
[11] R. Enberg, M.H. Reno and I. Sarcevic, *Phys. Rev. D.*, 78:043005 (2008).
[12] A.D. Martin, M.G. Ryskin and A.M. Stasto, *Acta Phys. Polon. B*, 34:3273 (2003).
[13] G. Fiorentini, A. Naumov and F.L. Villante, *Phys. Lett. B*, 510:173 (2001).
[14] G.J. Feldman and R.D. Cousins, *Phys. Rev. D.*, 57:3873 (1998).
[15] G.J. Feldman, "Multiple measurements and parameters in the unified approach," Workshop on Confidence Limits, Fermilab (2000).
[16] K. Cranmer, in *Statistical Problems in Particle Physics, Astrophysics and Cosmology: Proceedings of PHYSTAT05*, L. Lyons and M. Ünel, eds., (Univ. of Oxford, U.K., 2005);*arXiv:physics/0511028v2*.
[17] R. Brun and F. Rademakers, *Phys. Res. A*, 389:81 (1997).
[18] P. Adamson *et al.* , *Phys. Rev. Lett.*, 101:151601 (2008).
[19] R. Abbasi *et al.* , *arXiv:0902.0675v1*.